Mechanical stretch regulates microRNA expression profile via NF-κB activation in C2C12 myoblasts

WENXI HUA[1], MAHUI ZHANG[2], YONGKUI WANG[1], LEI YU[1], TINGTING ZHAO[1], XIAOZHONG QIU[1] and LEYU WANG[1]

[1]Department of Anatomy, Guangdong Provincial Key Laboratory of Construction and Detection in Tissue Engineering; [2]Department of Neurology, Zhujiang Hospital, Southern Medical University, Guangzhou, Guangdong 510515, P.R. China

Received September 13, 2015; Accepted September 23, 2016

DOI: 10.3892/mmr.2016.5907

Abstract. MicroRNAs (miRNAs/miRs) and nuclear factor (NF)-κB activation are involved in mechanical stretch-induced skeletal muscle regeneration. However, there are a small number of miRNAs that have been reported to be associated with NF-κB activation during mechanical stretch-induced myogenesis. In the present study, C2C12 myoblasts underwent cyclic mechanical stretch *in vitro*, to explore the relationship between miRNA expression and NF-κB activation during stretch-mediated myoblast proliferation. The results revealed that 10% deformation, 0.125 Hz cyclic mechanical stretch could promote myoblast proliferation. The miRNA expression profile was subsequently altered; miR-500, -1934, -31, -378, -331 and -5097 were downregulated, whereas miR-1941 was upregulated. These miRNAs were all involved in stretch-mediated myoblast proliferation. Notably, the expression of these miRNAs was reversed following treatment of 0.125 Hz mechanically stretched C2C12 cells with NF-κB inhibitors, which was accompanied by C2C12 cell growth suppression. Therefore, the present study is the first, to the best of our knowledge, to demonstrate that the NF-κB-dependent miRNA profile is associated with mechanical stretch-induced myoblast proliferation.

Introduction

In recent years, the incidence of skeletal muscle injury has increased. It is well known that skeletal muscles only possess limited self-renewal capacity. Skeletal muscles respond to mechanical load, and this mechanical stimulation has been reported to promote myogenesis by provoking muscle precursor cell activation, proliferation and differentiation (1). In the field of regenerative medicine, appropriate mechanical stimulation has been applied to muscle-derived stem cells in order to promote skeletal muscle repair (2). Furthermore, it has been suggested that external mechanical stimuli are transformed into intracellular signals through certain mechanisms, in order to regulate myoblast activity (3,4). However, the mechanisms underlying the transformation of external mechanical stimuli into intracellular signals remain unclear.

Nuclear factor (NF)-κB, which belongs to the Rel family, refers to several transcription factors. The mammalian NF-κB family comprises seven members, including p65 (RelA), c-Rel, RelB, p50/p105 (NF-κB1) and p52/p100 (NF-κB2). NF-κB usually exists in the form of hetero- or homodimers, and the typical NF-κB complex is composed of a p50 and p65 heterodimer. In non-stimulated cells, the NF-κB complex is located in the cytoplasm and is inhibited by the inhibitor of NF-κB (I-κBα). Once stimulated, the degradation of I-κBα and phosphorylation of NF-κB induce the translocation of NF-κB into the nucleus where it binds to target DNA (5). The translocation of NF-κB has been reported to regulate several cellular processes, including immunity and inflammation, cellular proliferation and differentiation (6-8). The role of NF-κB is indispensable and complex due to its presence in both proliferation and differentiation stages during the myogenic process (9). As for stretch-induced skeletal muscle alterations, the NF-κB signaling pathway has been shown to be activated in murine diaphragm muscles subjected to longitudinal mechanical stretch, resulting in upregulated expression of the stretch-response gene, Ankyrin repeat domain 2 (10). NF-κB activation by phosphorylation of p65 NF-κB has also been detected during cyclic stretch-induced myogenic differentiation (11). A previous study revealed that NF-κB transcriptional activity is beneficial to myoblast proliferation under appropriate stretch induction (12).

MicroRNAs (miRNAs/miRs) are small non-coding RNAs, some of which are highly evolutionarily conserved. miRNAs regulate gene expression at the post-transcriptional level by inhibiting translation of target mRNA or promoting target mRNA degradation (13). miRNAs have been identified as novel components in the gene regulatory network of myogenesis (14). A previous study reported that miRNAs are essential for the generation and maintenance of skeletal

Correspondence to: Dr Leyu Wang, Department of Anatomy, Guangdong Provincial Key Laboratory of Construction and Detection in Tissue Engineering, 11 Floor, Life Science Building, Southern Medical University, 1838 North Guanzhou Avenue, Baiyun, Guangzhou, Guangdong 510515, P.R. China
E-mail: wangleyu889@163.com

Key words: mechanical stretch, microRNAs, nuclear factor-κB, myoblasts, myogenesis

muscles (15). In particular, miRNAs specifically expressed in muscles, including miR-1 and miR-206, are able to promote skeletal myoblast differentiation (16,17). Conversely, another muscle-specific miRNA, miR-133, serves an opposite role in myogenesis by maintaining myoblasts in a proliferative state (16). Furthermore, local injection of miR-1, miR-133 and miR-206 can upregulate myogenin and myogenic differentiation 1 (MyoD) expression in injured skeletal muscles, and thus accelerates muscle regeneration (18). miRNAs that are ubiquitously expressed can also influence skeletal muscle development. miR-181 inhibits skeletal myogenesis, whereas miR-146a and miR-26a positively regulate myogenesis (19-21). However, interactions between the NF-κB signaling pathway and miRNAs during mechanical stretch-induced myoblast proliferation and differentiation remain unclear.

The present study subjected C2C12 myoblasts to cyclic stretch to investigate the interactions between NF-κB activation and miRNA expression during mechanical stretch-induced myoblast proliferation. The study focused on the myoblast proliferation process, since it represents the early stages of muscle regeneration. The computer-controlled Flexcell system was used to apply cyclic mechanical strain to C2C12 myoblasts. The appropriate mechanical stretch conditions that could promote C2C12 myoblast proliferation were initially confirmed, and the miRNA expression alterations during mechanical stretch-induced myoblast proliferation were determined using high-throughout sequencing and reverse transcription-quantitative polymerase chain reaction (RT-qPCR) methods. In addition, the interactions between NF-κB activation and miRNA expression were explored by treating stretch-induced myoblasts with or without an NF-κB inhibitor.

Materials and methods

Cell culture. C2C12 mouse myoblast cells were purchased from American Type Culture Collection (Manassas, VA, USA). The frozen stock was thawed and maintained as monolayer cultures in Dulbecco's modified Eagle's medium supplemented with 10% fetal bovine serum (both Gibco; Thermo Fisher Scientific, Inc., Waltham, MA, USA), 100 U/ml penicillin and 1,000 U/ml streptomycin at 37˚C in a humidified atmosphere containing 5% CO_2. The medium was changed twice per week.

Mechanical stretch stimulation of C2C12 cells. The model of *in vitro* stretching of C2C12 myoblasts was established using the computer-controlled vacuum stretch system (FX-5000 Tension system; FlexCell International Corporation, Burlington, NC, USA). Briefly, C2C12 cells were seeded into type-I collagen-coated flexible-bottom six-well plates (BioFlex collagen I plates; FlexCell International Corporation) at a density of $1x10^5$ cells/well in culture medium. The cells in the flexible-bottom six-well plates were then incubated at 37˚C in a humidified 5% CO_2 atmosphere overnight. Subsequently, C2C12 cells underwent cyclic strain (10% deformation) at 0.125, 0.25 and 0.5 Hz for 2 h per day for 4 consecutive days. Cells cultured under the same conditions without cyclic strain were considered the control group.

Cell viability assay and cell cycle analysis. C2C12 cell viability was assessed 1, 2, 3 and 4 days after initiation of cyclic strain using the Cell Counting kit-8 (CCK-8) assay. Briefly, C2C12 cells in the control group, and 0.125, 0.25 and 0.5 Hz groups were digested with 0.25% pancreatic enzyme (trypsin; Gibco; Thermo Fisher Scientific, Inc.) containing 0.02% EDTA. The cells were then reseeded in 96-well plates at a density of $5x10^3$ cells/well in culture medium (8 duplicate wells/group). The plates were incubated for 24 h at 37˚C, after which the cell medium was replaced with 100 μl culture medium containing 10 μl CCK-8 reagent (Dojindo Molecular Technologies, Inc., Kumamoto, Japan). Following a further incubation for 3 h at 37˚C, the optical density (OD) values were measured at 450 nm using a microplate reader (Thermo Fisher Scientific, Inc.). Cell cycle analysis was performed by flow cytometry (FCM). Briefly, stretched C2C12 cells (10% deformation; 0.125 Hz) at day 4 and control cells were collected. Subsequently, the cells were permeabilized with 70% (v/v) ethanol and incubated overnight at 4˚C. Finally, the cells were stained with 500 μl propidium iodide (100 μg/ml) at 37˚C for 30 min and analyzed by FCM. The relative DNA proliferation index (DPI) was calculated using the following formula: [DPI = (S% + G_2 / M%) / (S% + G_2 / M% + G_0 / G_1%)], according to our previous report (7).

High-throughput sequencing. High-throughput sequencing was applied to detect differentially expressed miRNAs in C2C12 cells between the control group and the 0.125 Hz stretch group at day 4. Total RNA was extracted from the C2C12 cells using TRIzol® (Invitrogen; Thermo Fisher Scientific, Inc.) according to the manufacturer's protocol. Small RNAs (18-75 nt) were separated from total RNAs by polyacrylamide gel electrophoresis and were purified. The small RNAs were ligated with 5' and 3' adapters using T4 RNA Ligase (Thermo Fisher Scientific, Inc.), and were reverse transcribed to cDNA using SuperScript II (Life Technologies; Thermo Fisher Scientific, Inc.). Generation of double-stranded cDNA was performed prior to PCR amplification. High-throughput sequencing of the purified DNA samples was performed using the Illumina Genome Analyzer IIx (Illumina, San Diego, CA, USA). To select differentially expressed miRNAs between the two groups, the frequency of miRNAs was normalized to calculate the ratio of 0.125 Hz stretched cells to control cells. A differentially expressed miRNA was indicated by a stretched/control ratio >2 and a statistically significant result, as determined by independent t-test with Bonferroni correction.

NF-κB inhibition. Two selective and irreversible NF-κB inhibitors: BAY11-7082 (BAY; Beyotime Institute of Biotechnology, Jiangsu, China) and pyrrolidine dithiocarbamate (PDTC; Beyotime Institute of Biotechnology) were used in the present study. In order to determine the effects of NF-κB inhibition on the stretched myoblasts, C2C12 cells that underwent 0.125 Hz cyclic strain (10% deformation) for 2 h per day for 4 consecutive days were simultaneously treated with 2.5 μM BAY, 5 μM BAY or 10 μM PDTC. The effects of NF-κB inhibition on stretched C2C12 myoblasts were subsequently detected according to the aforementioned CCK-8 method and FCM analysis at corresponding time points.

Western blot analysis. Cells were lysed with radioimmunoprecipitation assay buffer (EMD Millipore, Billerica, MA, USA) and protein concentration was determined using the

bicinchoninic acid assay kit (Thermo, Fisher Scientific, Inc.). Protein samples (50 μg) were separated by SDS-PAGE (5% stacking gel, 10% separating gel), and were then transferred to polyvinylidene fluoride (PVDF) membranes (Bio-Rad Laboratories, Inc., Hercules, CA, USA). The membranes were then rinsed with TBS-0.05% Tween-20 (TBST) and blocked with 5% fat-free dried milk solution at room temperature for 1.5 h. Primary antibodies: Rabbit anti-NF-κB (ab16502; 1:2,000), rabbit anti-phosphorylated (P)-NF-κB (ab86299; 1:1,000), mouse anti-I-κBα (ab211340; 1:1,000) and mouse anti-GAPDH (ab8245; 1:2,000) (all Abcam, Cambridge, MA, USA) were added, and the membranes were incubated overnight at 4˚C. Subsequently, the PVDF membranes were rinsed 3 times with TBST (5 min/wash) and were incubated with horseradish peroxidase-conjugated goat anti-mouse IgG (ab97023; 1:3,000 and 1:5,000 for anti-I-κBα and anti-GAPDH primary antibodies, respectively) and goat anti-rabbit IgG (ab6721; 1:5,000 and 1:3,000 for anti-NF-κB and anti-P-NF-κB primary antibodies, respectively) secondary antibodies from Abcam, prior to visualization by enhanced chemiluminescence. Experiments were repeated three times. Relative expression levels were determined using ImageJ software, version 2.1.4.7 (National Institutes of Health, Bethesda, MD, USA) and were normalized to loading controls.

RT-qPCR. Total RNA was extracted from C2C12 cells in the control group, 0.125 Hz stretch group and NF-κB inhibitor + 0.125 Hz stretch group at day 4 using TRIzol® according to the manufacturer's protocol. RT was performed using an ABI 9700 PCR amplification machine (Applied Biosystems; Thermo Fisher Scientific, Inc.) and a miR RT kit (Takara Bio, Inc., Otsu, Japan). Briefly, aliquots (2 μg) of total RNA were transcribed into cDNA in a total volume of 20 μl with 5X PrimeScript buffer, 1 mmol/l nucleotide mixture, 50 pmol/l primer, 100 U PrimeScript Reverse Transcriptase, and 20 U RNase inhibitor. The RT reaction was conducted at 37˚C for 15 min, 85˚C for 5 sec and 4˚C prior to qPCR analysis. qPCR was performed in triplicate using a PCR detection system (Stratagene Mx3000P qPCR system; Agilent Technologies, Santa Clara, CA, USA). miRNA specific primer sequences are listed in Table I. All primers were synthesized by Guangzhou Vipotion Biotechnology Co., Ltd. (Guangzhou, China). qPCR was conducted using the *Taq* PCR kit (Takara Bio, Inc.) in a 20 μl reaction volume containing 2 μl miRNA RT product, 0.2 μl 1 U/μl *Taq* DNA polymerase, 10 μl 5X PCR Buffer, 0.6 μl 5 μM primer and deionized water. Reaction conditions were as follows: Initial denaturation at 95˚C for 3 min, 40 cycles of 95˚C for 12 sec and 62˚C for 60 sec, followed by an extension step at 72˚C for 1 min. The relative miRNA expression levels were calculated using the comparative threshold cycle $2^{-\Delta\Delta Cq}$ method (22).

Statistical analysis. Data were analyzed by one-way analysis of variance and the post-hoc Bonferroni test was used for pair-wise comparisons. Statistical analyses were performed using SPSS 19.0 (IBM SPSS, Armonk, NY, USA) and the data were presented as the mean ± standard deviation, error bars were representative of three independent experiments. P<0.05 was considered to indicate a statistically significant difference.

Table I. miR specific primer sequences.

Primer name	Sequence (5'-3')
mmu-mir-500	AAUGCACCUGGGCAAGGGUUCA
mmu-mir-1934	AGGAUGACGGUGGGGCUGGUGA
mmu-mir-31	AGGCAAGAUGCUGGCAUAGCUG
mmu-mir-378a	ACUGGACUUGGAGUCAGAAGG
mmu-mir-331	GCCCCUGGGCCUAUCCUAGAA
mmu-mir-5097	GUUCAUGUCCCUGUUCAGGCGCCA
mmu-mir-1941	AGGGAGAUGCUGGUACAGAGGCUU

miR, microRNA.

Results

Alterations to the miRNA expression profile during mechanical stretch-induced myoblast proliferation. To investigate the effects of various stretch frequencies on myoblast viability, the CCK-8 assay was performed 1, 2, 3 and 4 days after the cells underwent cyclic stretching. At day 3, the mean OD value of the 0.125 Hz stretch group (10% deformation) was significantly higher compared with in the control group; 1.65 vs. 0.71 respectively (P<0.05; Fig. 1A). At day 4, the mean OD value of the 0.125 Hz stretched cells remained higher compared with the control cells; 1.63 vs. 0.81 (P<0.05). Furthermore, cell cycle progression differed between the control cells and the 0.125 Hz stretched myoblasts (10% deformation) at day 4. As shown in Fig. 1B, the number of cells in the proliferative (S or G_2) phase was markedly higher in the 0.125 Hz stretch group compared with in the control group. At day 4, the mean DPI in the 0.125 Hz stretch group was significantly increased compared with in the control cells (Fig. 1B). These results suggest that 10% deformation cyclic strain at 0.125 Hz can enhance myoblast viability and stimulate myoblast entry into the proliferative phase, thus promoting C2C12 cell proliferation. Conversely, 10% deformation cyclic strain at 0.5 Hz markedly inhibited C2C12 cell viability at day 4 compared with the control (Fig. 1A). Therefore, 10% deformation cyclic mechanical stretch at 0.125 Hz were considered the appropriate stretch conditions.

Alterations to the miRNA profile between the control group and the 0.125 Hz mechanical stretch group were determined by high-throughput sequencing. The hierarchical clustering analysis of differentially expressed miRNAs is presented in Fig. 2. Within the miRNA expression profiles, 10 miRNAs exhibited >2-fold variation in the 0.125 Hz mechanical stretch group compared with in the control group. Seven (miR-500, -1934, -31, -378a, -3473b, -331 and -5097) of which were downregulated, whereas three (miR-340, -449c and -1941) were upregulated in the mechanical stretch group (Fig. 3A). Among them, miR-500, miR-1934, miR-31, miR-378a, miR-331, miR-5097 and miR-1941, were validated through the RT-qPCR method (Fig. 3B).

Differentially expressed miRNAs induced by cyclic mechanical stretch are reversed by NF-κB inhibition in C2C12 myoblasts. The present study aimed to explore the association

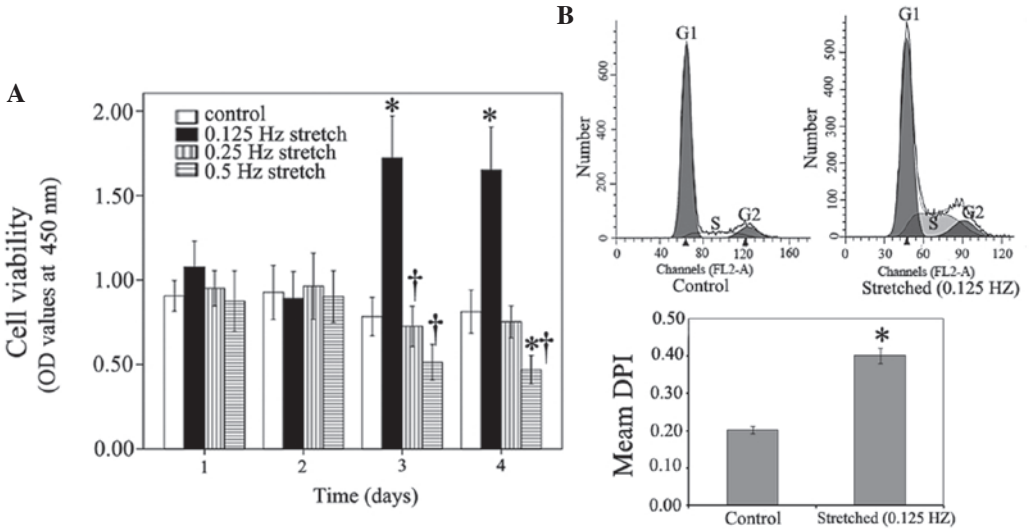

Figure 1. Appropriate mechanical stretch promotes myoblast proliferation. (A) Effects of mechanical stretch frequency on the viability of C2C12 cells, as detected by Cell Counting kit-8 assay. (B) Flow cytometric analysis of cell cycle progression in 0.125 Hz stretched myoblasts and control cells at day 4. *P<0.05 vs. the control group. †P<0.05 vs. the 0.125 Hz group. n=3. OD, optical density; DPI, DNA proliferation index.

between NF-κB activation and miRNA expression during stretch-induced myoblast proliferation. As shown in Fig. 4A, 0.125 Hz mechanical stretch increased the expression levels of NF-κB p65 and P-NF-κB p65, whereas the expression levels of the inhibitory factor I-κBα were decreased compared with the control group (P<0.05). However, treatment with 2.5 or 5 μM NF-κB inhibitor BAY inhibited NF-κB p65 and P-NF-κB p65 expression, and increased the expression levels of I-κBα compared with the stretch group. Treatment with 5 μM BAY resulted in a more significant inhibition of NF-κB activation (P<0.05). These results suggest that NF-κB is activated in the process of stretch-mediated myoblast proliferation, and the NF-κB inhibitor BAY can effectively inhibit activation of NF-κB p65 in stretched C2C12 cells.

Compared with 2.5 μM BAY, 5 μM BAY displayed an increased inhibitory effect on NF-κB activation. Therefore, 5 μM BAY was selected as the dose for NF-κB inhibition in subsequent experiments regarding miRNA expression. As shown in Fig. 4B, 0.125 Hz stretch-induced downregulation of miR-500, miR-1934, miR-31 and miR-378a in C2C12 cells was reversed by 5 μM BAY. Furthermore, 0.125 Hz stretch-induced reduced expression of miR-331 and miR-5097 was significantly reversed by 5 μM BAY (P<0.05). Conversely, the 0.125 Hz mechanical stretch-induced expression of miR-1941 was significantly reduced following treatment with 5 μM BAY (P<0.05). These data indicate that 5 μM Bay can reverse mechanical stretch-induced miRNA expression alterations.

The effects of the NF-κB inhibitor BAY were also determined on mechanical stretch-induced myoblast proliferation, as assessed by CCK-8 assay and FCM. The 0.125 Hz mechanical stretch-induced increased OD value was significantly decreased in C2C12 cells following treatment with 2.5 μM BAY on days 2, 3 and 4. Treatment with 5 μM BAY was able to inhibit stretched myoblast viability on the first day, and sustain the inhibitory effect between days 2 and 4 (P<0.05; Fig. 5A). FCM revealed that stretched C2C12 cells treated with 5 μM BAY were arrested in G_1 phase at day 4, and the mean DPI in stretched C2C12 cells treated with 5 μM BAY was significantly decreased compared with the control cells (P<0.05; Fig. 5B). These results suggest that the NF-κB inhibitor BAY may inhibit stretch-induced myoblast proliferation.

The present study used another NF-κB inhibitor, PDTC, to confirm the effects of NF-κB inhibition on stretched myoblasts. The results, as shown in Fig. 6, revealed that 10 μM PDTC elicited similar effects to BAY. Treatment of C2C12 cells with 10 μM PDTC inhibited activation of NF-κB, reversed alterations in stretch-induced miRNA expression and inhibited stretch-induced myoblast proliferation.

Discussion

Variations in the duration, magnitude and frequency of mechanical stretch have discrepant influences on myoblasts. Appropriate external mechanical stimulation can promote the proliferation of myoblasts cultured *in vitro* (23,24). In addition, it has previously been reported that mechanical stretch (15% strain) may induce conspicuous injury to muscle cells (25), whereas cyclic tensile stretch (10% strain) at 1 Hz for 1 h followed by 23 h of relaxation could enhance myoblast proliferation (24). The results of the present study revealed that only 0.125 Hz mechanical stretch could promote myoblast proliferation when C2C12 myoblasts were exposed to 10% tensile cyclic strain at various frequencies (0.125, 0.25 and 0.5 Hz). Similar findings have been reported in human bladder smooth muscle cells cultured *in vitro*; 5% equibiaxial stretch at 0.1 Hz promoted smooth muscle cell proliferation and decreased apoptotic rate (25).

In the present study, seven mechanical stretch-associated miRNAs were detected in C2C12 cells: MiR-500, miR-1934, miR-31, miR-378a, miR-331, miR-5097 and miR-1941, which were identified using high-throughput sequencing and RT-qPCR analysis. Among them, miR-500 has previously been detected in the dorsal root ganglia of rats and is thought to be involved in nerve reconstruction (26). Furthermore, miR-31

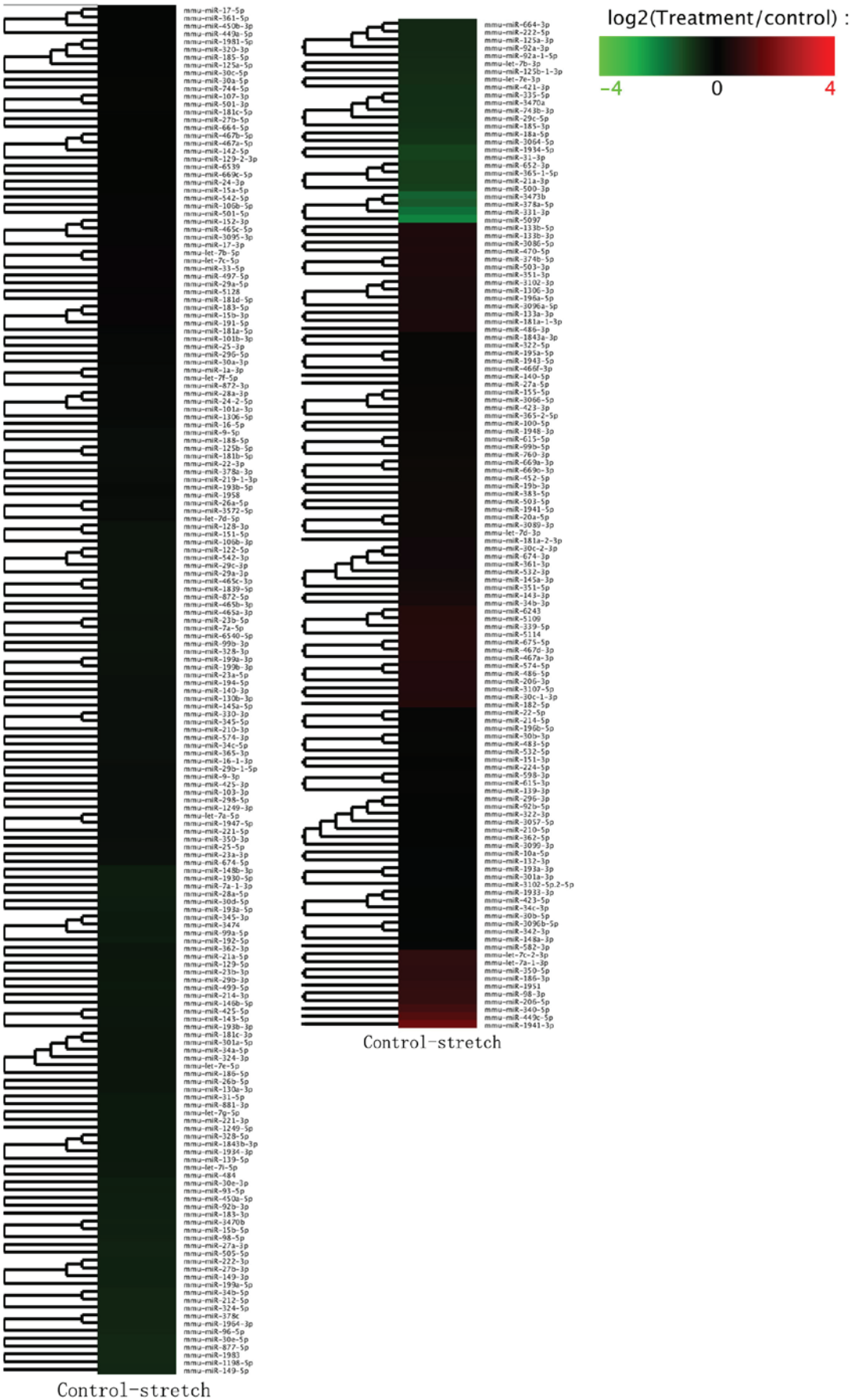

Figure 2. Hierarchical clustering analysis of the log2 values of differentially expressed miRs between the 0.125 Hz mechanical stretch group and the control group. Green color indicates downregulated expression in the mechanical stretch group compared with in the control group; red color indicates upregulated expression in the mechanical stretch group compared with in the control group; black color indicates no significant difference in the expression between the two groups. miR, microRNA.

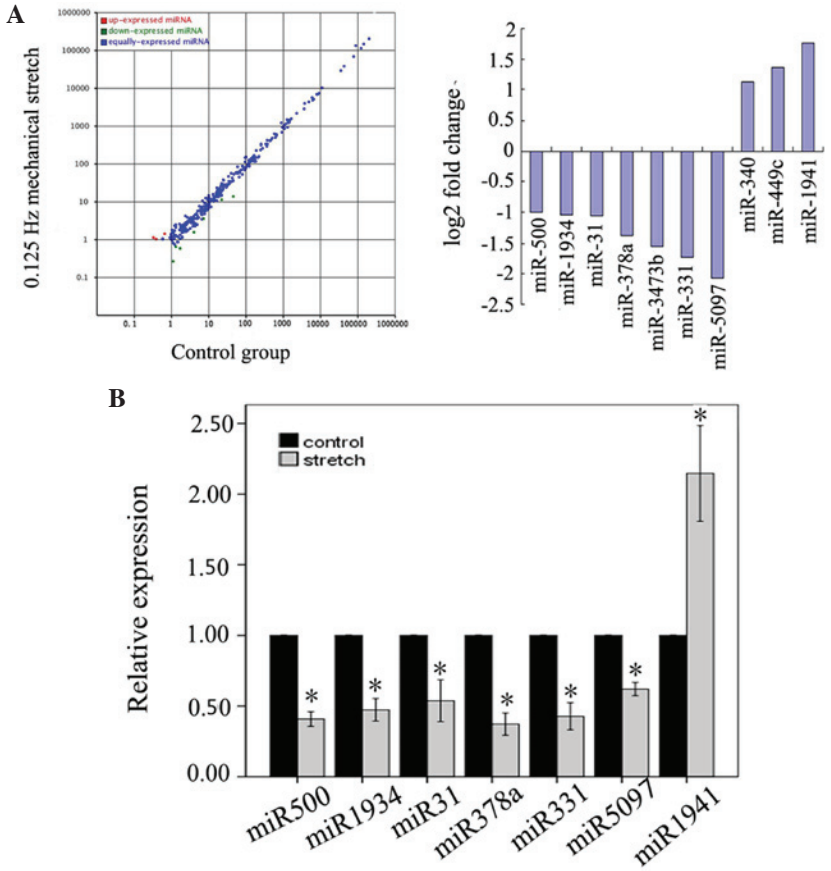

Figure 3. (A) Differentially expressed miRNAs in the 0.125 Hz mechanical stretch group compared with the control group. (B) Relative expression levels of miR-500, miR-1934, miR-31, miR-378, miR-331, miR-5097 and miR-1941 in the control and 0.125 Hz mechanical stretch groups. The expression levels in the 0.125 Hz mechanical stretch group were normalized to the control group. *P<0.05 vs. the control group. n=3. miR, microRNA.

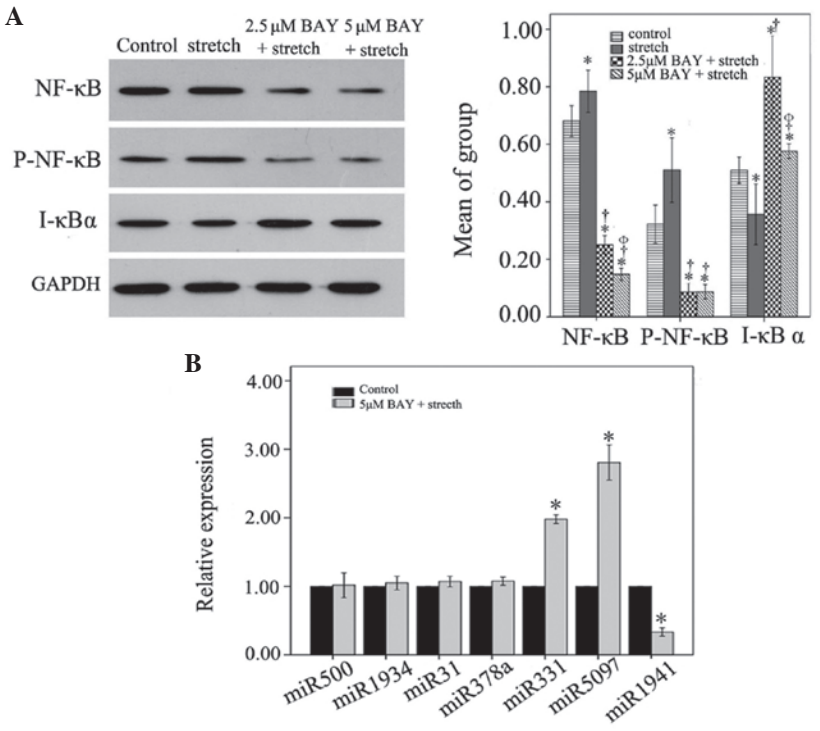

Figure 4. (A) Effects of NF-κB inhibition on the expression levels of NF-κB p65, P-NF-κB p65, and I-κBα proteins in 0.125 Hz stretched C2C12 cells. *P<0.05 vs. the control group. †P<0.05 vs. the stretch group. ΦP<0.05 vs. the 2.5 μM BAY group. n=3. (B) Relative expression levels of miR-500, miR-1934, miR-31, miR-378, miR-331, miR-5097 and miR-1941 in control and 5 μM BAY + mechanical stretch groups. Expression levels in the 5 μM Bay + 0.125 Hz mechanical stretch group were normalized to the control group. *P<0.05 vs. the control group. n=3. miR, microRNA; NF-κB, nuclear factor-κB; P-, phosphorylated; I-κBα, inhibitor of NF-κB; BAY, BAY11-7082.

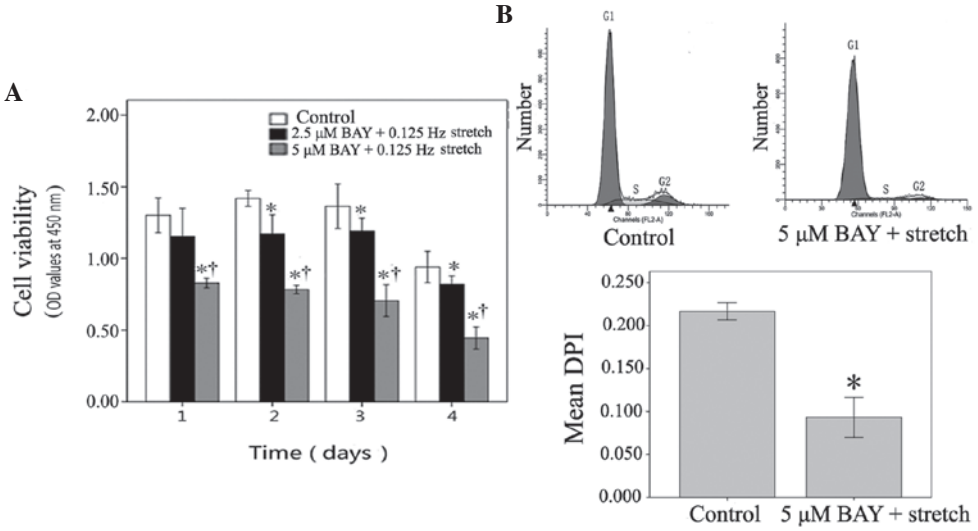

Figure 5. NF-κB inhibitor BAY inhibits stretch-induced C2C12 cell proliferation. (A) Effects of NF-κB inhibition on the viability of 0.125 Hz-stretched C2C12 cells, as detected by Cell Counting kit-8 assay. *P<0.05 vs. the control group. †P<0.05 vs. the 2.5 μM BAY group. (B) Flow cytometric analysis of cell cycle progression in stretched myoblasts treated with 5 μM BAY and control cells at day 4. *P<0.05 vs. the control group. n=3. NF-κB, nuclear factor-κB; BAY, BAY11-7082; DPI, DNA proliferation index.

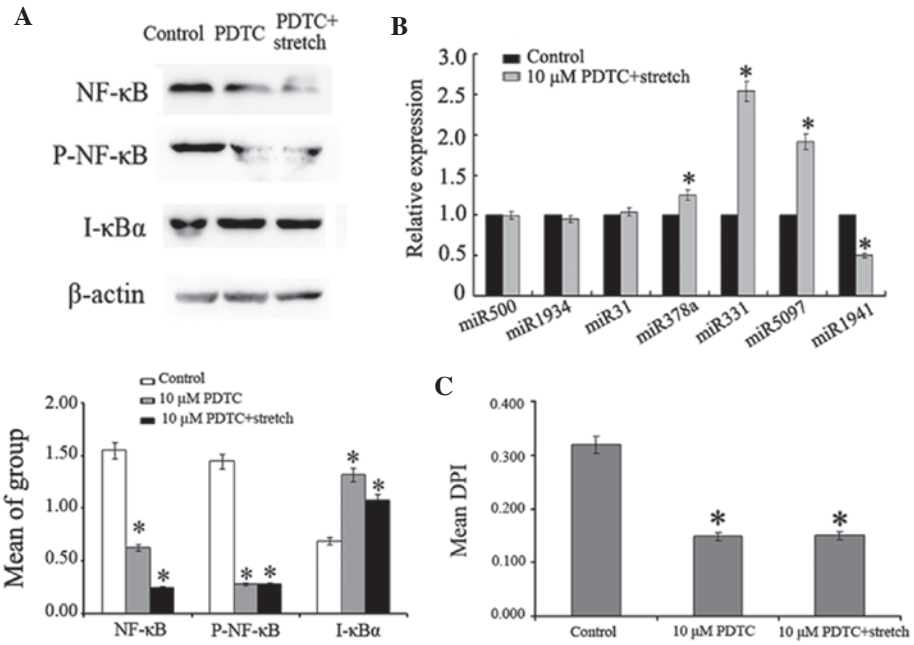

Figure 6. (A) Effects of 10 μM PDTC on the expression levels of NF-κB p65, P-NF-κB p65 and I-κBα proteins in 0.125 Hz stretched C2C12 cells, as detected by western blotting. (B) Relative expression levels of miR-500, miR-1934, miR-31, miR-378, miR-331, miR-5097 and miR-1941 in control and 10 μM PDTC + mechanical stretch groups. (C) Effects of 10 μM PDTC on 0.125 Hz stretch-induced myoblast proliferation. *P<0.05 vs. the control group. n=3. miR, microRNA; NF-κB, nuclear factor-κB; P-, phosphorylated; I-κBα, inhibitor of NF-κB; PDTC, pyrrolidine dithiocarbamate; DPI, DNA proliferation index.

is able to promote the expression of myogenic factor 5 and myoblast proliferation. Targeted inhibition of miR-31 has been reported to be an effective therapeutic strategy for dystrophin rescue in human Duchenne muscular dystrophy (27,28). In addition, miR-378 may suppress proliferation of myoblasts by modulating the mitogen-activated protein kinases (MAPK) pathway and bone morphogenetic proteins (29,30). The over-expression of miR-378 promotes myoblast differentiation by strengthening MyoD activity (30). Increased expression of miR-331 has also been detected during myoblast differentiation (31). These findings are similar to the results of the present study; the expression levels of miR-31, miR-378 and miR-331 were reduced during the process of 10% strain, 0.125 Hz mechanical stretch-induced myoblast proliferation. In addition, to the best of our knowledge, miR-1941, miR-1934, miR-5097 and miR-500 may be considered novel candidates for stretch-induced myogenesis, which have not been reported previously.

The present study further explored the effects of NF-κB, which participates in the enhanced proliferative process elicited by mechanical stretch. There are several signaling pathways associated with mechanical stretch in skeletal muscle cells,

including protein kinase C (32), MAPK (33), phosphatidylinositol-3 kinase/Akt (34), NF-κB (12), calcineurin (35) and nitric oxide synthase (36). However, findings published over the past few years have suggested that these signaling pathways have a close connection and serve crosstalk roles in inflammatory and immune responses (37-39). Notably, MAPK appears to be an upstream regulator of the NF-κB signaling pathway, which can successfully induce NF-κB-dependent myogenesis (8-11). In the present study, the NF-κB signaling pathway was activated by mechanical stretch, as determined by the markedly increased protein expression levels of NF-κB p65 and P-NF-κB p65. Following treatment with NF-κB inhibitors, translocation of NF-κB in stretch-loaded myoblasts was inhibited, which was accompanied by the reversal of miRNA expression and the suppression of proliferation in C2C12 myoblasts. Therefore, these results indicated that the NF-κB signaling pathway is activated and exerts direct effects in stretch-induced myoblasts. These results are concordant with the findings reported by Kumar *et al*, which indicated that NF-κB is indispensable for stretch-induced proliferation of C2C12 cells (12).

The results of the present study identified a link between NF-κB and miRNA expression. The expression levels of miR-500, miR-1934, miR-31, miR-378a, miR-331 and miR-5097 were downregulated in myoblasts following mechanical stretch, whereas NF-κB inhibition increased the expression of these miRNAs. Conversely, the upregulation of miR-1941 was markedly reduced by NF-κB inhibition in mechanically stretched C2C12 cells. Similarly, bioinformatics analysis in a previous study suggested the presence of an NF-κB binding element in the promoter region of miR-26a; inhibition of NF-κB in cardiac fibroblasts increased miR-26a expression, whereas overexpression of miR-26a inhibited NF-κB activity, thus indicating a feedback loop in cardiac fibroblasts (40). The results of the present study are the first, to the best of our knowledge, to reveal that miRNA expression is NF-κB-dependent during stretch-induced myoblast proliferation, thus suggesting a possible mechanism regarding the transformation of external mechanical stimuli into intracellular signals.

The present study used two structurally different NF-κB inhibitors in order to confirm the effects of the NF-κB signaling pathway on stretched myoblasts. BAY is a specific inhibitor of NF-κB, due to its inhibitory effect on the activation of NF-κB and the phosphorylation of I-κBα (41). PDTC is able to inhibit activation of NF-κB specifically by suppressing the release of the inhibitory subunit I-κB from the latent cytoplasmic form of NF-κB (42-44). The results of the present study revealed that the two NF-κB inhibitors were able to inhibit activation of NF-κB, reverse stretch-induced miRNA profile alterations in C2C12 myoblasts, and suppress stretch-induced myoblast proliferation. Accordingly, these data confirmed the interaction between miRNAs and the NF-κB signaling pathway during stretch-induced myogenesis.

In conclusion, cyclic stretch (10% deformation; 0.125 Hz) was able to activate the NF-κB signaling pathway, reduce the expression levels of miR-500, -1934, -31, -378, -331 and -5097, increase the expression of miR-1941, and promote proliferation of C2C12 cells. However, treatment with NF-κB inhibitors inhibited NF-κB activation in mechanically stretched C2C12 cells, which was accompanied by reversed expression of miRNAs and suppressed cell proliferation. These results demonstrated that cyclic stretch-mediated cell proliferation and miRNA profile alterations in C2C12 myoblasts occur via activation of the NF-κB signaling pathway, thus providing a possible mechanism during stretch-induced myogenesis.

Acknowledgements

The present study was supported by the National Natural Science Foundation of China (grant no. 31100700) and the Guangdong Medical Research Foundation (grant no. A2015412).

References

1. Tidball JG: Mechanical signal transduction in skeletal muscle growth and adaptation. J Appl Physiol (1985) 98: 1900-1908, 2005.
2. Beckman SA, Chen WC, Tang Y, Proto JD, Mlakar L, Wang B and Huard J: Beneficial effect of mechanical stimulation on the regenerative potential of muscle-derived stem cells is lost by inhibiting vascular endothelial growth factor. Arterioscler Thromb Vasc Biol 33: 2004-2012, 2013.
3. Klumpp D, Horch RE, Kneser U and Beier JP: Engineering skeletal muscle tissue-new perspectives in vitro and in vivo. J Cell Mol Med 14: 2622-2629, 2010.
4. Ross TD, Coon BG, Yun S, Baeyens N, Tanaka K, Ouyang M and Schwartz MA: Integrins in mechanotransduction. Curr Opin Cell Biol 25: 613-618, 2013.
5. Kurihara Y and Furue M: Interferon-gamma enhances phorbol myristate acetate-induced cell attachment and tumor necrosis factor production via the NF-kB pathway in THP-1 human monocytic cells. Mol Med Rep 7: 1739-1744, 2013.
6. Karin M and Ben-Neriah Y: Phosphorylation meets ubiquitination: The control of NF-[kappa]B activity. Annu Rev Immunol 18: 621-663, 2000.
7. Wang LY, Wang HY, Ouyang J, Yu L, Chen B, Qin JQ and Qiu XZ: Low concentration of lipopolysaccharide acts on MC3T3-E1 osteoblasts and induces proliferation via the COX-2-independent NFkappaB pathway. Cell Biochem Funct 27: 238-242, 2009.
8. Baeza-Raja B and Muñoz-Cánoves P: p38 MAPK-induced nuclear factor-kappaB activity is required for skeletal muscle differentiation: Role of interleukin-6. Mol Biol Cell 15: 2013-2026, 2004.
9. Bakkar N and Guttridge DC: NF-kappaB signaling: A tale of two pathways in skeletal myogenesis. Physiol Rev 90: 495-511, 2010.
10. Mohamed JS, Lopez MA, Cox GA and Boriek AM: Anisotropic regulation of Ankrd2 gene expression in skeletal muscle by mechanical stretch. FASEB J 24: 3330-3340, 2010.
11. Ji G, Liu D, Liu J, Gao H, Yuan X and Shen G: p38 mitogen-activated protein kinase up-regulates NF-kappaB transcriptional activation through RelA phosphorylation during stretch-induced myogenesis. Biochem Biophys Res Commun 391: 547-551, 2010.
12. Kumar A, Murphy R, Robinson P, Wei L and Boriek AM: Cyclic mechanical strain inhibits skeletal myogenesis through activation of focal adhesion kinase, Rac-1 GTPase, and NF-kappaB transcription factor. FASEB J 18: 1524-1535, 2004.
13. Wang K, Xu Z, Wang N, Tian Y, Sun X and Ma Y: Analysis of microRNA and gene networks in human chronic myelogenous leukemia. Mol Med Rep 13: 453-460, 2016.
14. Wang H, Sun H and Guttridge DC: microRNAs: Novel components in a muscle gene regulatory network. Cell Cycle 8: 1833-1837, 2009.
15. O'Rourke JR, Georges SA, Seay HR, Tapscott SJ, McManus MT, Goldhamer DJ, Swanson MS and Harfe BD: Essential role for Dicer during skeletal muscle development. Dev Biol 311: 359-368, 2007.
16. Chen JF, Mandel EM, Thomson JM, Wu Q, Callis TE, Hammond SM, Conlon FL and Wang DZ: The role of microRNA-1 and microRNA-133 in skeletal muscle proliferation and differentiation. Nat Genet 38: 228-233, 2006.
17. Lu J, McKinsey TA, Zhang CL and Olson EN: Regulation of skeletal myogenesis by association of the MEF2 transcription factor with class II histone deacetylases. Mol Cell 6: 233-244, 2000.

18. Nakasa T, Ishikawa M, Shi M, Shibuya H, Adachi N and Ochi M: Acceleration of muscle regeneration by local injection of muscle-specific microRNAs in rat skeletal muscle injury model. J Cell Mol Med 14: 2495-2505, 2010.
19. Yamamoto M and Kuroiwa A: Hoxa-11 and Hoxa-13 are involved in repression of MyoD during limb muscle development. Dev Growth Differ 45: 485-498, 2003.
20. Kuang W, Tan J, Duan Y, Duan J, Wang W, Jin F, Jin Z, Yuan X and Liu Y: Cyclic stretch induced miR-146a upregulation delays C2C12 myogenic differentiation through inhibition of Numb. Biochem Biophys Res Commun 378: 259-263, 2009.
21. Wong CF and Tellam RL: MicroRNA-26a targets the histone methyltransferase Enhancer of Zeste homolog 2 during myogenesis. J Biol Chem 283: 9836-9843, 2008.
22. Livak KJ and Schmittgen TD: Analysis of relative gene expression data using real-time quantitative PCR and the 2(-Delta Delta C(T)) Method. Methods 25: 402-408, 2001.
23. Otis JS, Burkholder TJ and Pavlath GK: Stretch-induced myoblast proliferation is dependent on the COX2 pathway. Exp Cell Res 310: 417-425, 2005.
24. Kook SH, Lee HJ, Chung WT, Hwang IH, Lee SA, Kim BS and Lee JC: Cyclic mechanical stretch stimulates the proliferation of C2C12 myoblasts and inhibits their differentiation via prolonged activation of p38 MAPK. Mol Cells 25: 479-486, 2008.
25. Wazir R, Luo DY, Dai Y, Yue X, Tian Y and Wang KJ: Expression and proliferation profiles of PKC, JNK and p38MAPK in physiologically stretched human bladder smooth muscle cells. Biochem Biophys Res Commun 438: 479-482, 2013.
26. Yu B, Zhou S, Qian T, Wang Y, Ding F and Gu X: Altered microRNA expression following sciatic nerve resection in dorsal root ganglia of rats. Acta Biochim Biophys Sin (Shanghai) 43: 909-915, 2011.
27. Crist CG, Montarras D and Buckingham M: Muscle satellite cells are primed for myogenesis but maintain quiescence with sequestration of Myf5 mRNA targeted by microRNA-31 in mRNP granules. Cell Stem Cell 11: 118-126, 2012.
28. Cacchiarelli D, Incitti T, Martone J, Cesana M, Cazzella V, Santini T, Sthandier O and Bozzoni I: miR-31 modulates dystrophin expression: New implications for Duchenne muscular dystrophy therapy. EMBO Rep 12: 136-141, 2011.
29. Hou X, Tang Z, Liu H, Wang N, Ju H and Li K: Discovery of MicroRNAs associated with myogenesis by deep sequencing of serial developmental skeletal muscles in pigs. PLoS One 7: e52123, 2012.
30. Jeon TI, Park JW, Ahn J, Jung CH and Ha TY: Fisetin protects against hepatosteatosis in mice by inhibiting miR-378. Mol Nutr Food Res 57: 1931-1937, 2013.
31. Dmitriev P, Barat A, Polesskaya A, O'Connell MJ, Robert T, Dessen P, Walsh TA, Lazar V, Turki A, Carnac G, *et al*: Simultaneous miRNA and mRNA transcriptome profiling of human myoblasts reveals a novel set of myogenic differentiation-associated miRNAs and their target genes. BMC Genomics 14: 265, 2013.
32. Nobe K and Paul RJ: Distinct pathways of Ca(2+) sensitization in porcine coronary artery: Effects of Rho-related kinase and protein kinase C inhibition on force and intracellular Ca(2+). Circ Res 88: 1283-1290, 2001.
33. Martineau LC and Gardiner PF: Insight into skeletal muscle mechanotransduction: MAPK activation is quantitatively related to tension. J Appl Physiol (1985) 91: 693-702, 2001.
34. Sakamoto K, Aschenbach WG, Hirshman MF and Goodyear LJ: Akt signaling in skeletal muscle: Regulation by exercise and passive stretch. Am J Physiol Endocrinol Metab 285: E1081-E1088, 2003.
35. Bassel-Duby R and Olson EN: Role of calcineurin in striated muscle: Development, adaptation, and disease. Biochem Biophys Res Commun 311: 1133-1141, 2003.
36. Tidball JG, Spencer MJ, Wehling M and Lavergne E: Nitric-oxide synthase is a mechanical signal transducer that modulates talin and vinculin expression. J Biol Chem 274: 33155-33160, 1999.
37. Parola C, Salogni L, Vaira X, Scutera S, Somma P, Salvi V, Musso T, Tabbia G, Bardessono M, Pasquali C, *et al*: Selective activation of human dendritic cells by OM-85 through a NF-kB and MAPK dependent pathway. PLoS One 8: e82867, 2013.
38. Hu H, Li Z, Zhu X, Lin R and Chen L: Salidroside reduces cell mobility via NF-k B and MAPK signaling in LPS-Induced BV2 microglial cells. Evid Based Complement Alternat Med 2014: 383821, 2014.
39. Hong GE, Kim JA, Nagappan A, Yumnam S, Lee HJ, Kim EH, Lee WS, Shin SC, Park HS and Kim GS: Flavonoids Identified from Korean Scutellaria baicalensis Georgi inhibit inflammatory signaling by suppressing activation of NF-kB and MAPK in RAW 264.7 cells. Evid Based Complement Alternat Med 2013: 912031, 2013.
40. Wei C, Kim IK, Kumar S, Jayasinghe S, Hong N, Castoldi G, Catalucci D, Jones WK and Gupta S: NF-kB mediated miR-26a regulation in cardiac fibrosis. J Cell Physiol 228: 1433-1442, 2013.
41. Moore LB, Sawyer AJ, Charokopos A, Skokos EA and Kyriakides TR: Loss of monocyte chemoattractant protein-1 alters macrophage polarization and reduces NFkB activation in the foreign body response. Acta Biomater 11: 37-47, 2015.
42. Guo RM, Xu WM, Lin JC, Mo LQ, Hua XX, Chen PX, Wu K, Zheng DD and Feng JQ: Activation of the p38 MAPK/NF-kB pathway contributes to doxorubicin-induced inflammation and cytotoxicity in H9c2 cardiac cells. Mol Med Rep 8: 603-608, 2013.
43. Huang T, Gao D, Jiang X, Hu S, Zhang L and Fei Z: Resveratrol inhibits oxygen-glucose deprivation-induced MMP-3 expression and cell apoptosis in primary cortical cells via the NF-kB pathway. Mol Med Rep 10: 1065-1071, 2014.
44. Li T, Zhang Q, Zhang J, Yang G, Shao Z, Luo J, Fan M, Ni C, Wu Z and Hu X: Fenofibrate induces apoptosis of triple-negative breast cancer cells via activation of NF-kB pathway. BMC Cancer 14: 96, 2014.